Supplementary Data

LUMINESCENCE DATING PROCEDURES AND PROTOCOLS

Sample preparation

Samples were prepared and analyzed at the Desert Research Institute Luminescence Laboratory (DRILL). Target 180-250 μm potassium feldspar (KF) grains were extracted from the bulk sediment samples using standard heavy liquid separation procedures (Aitken, 1998). Samples were deflocculated using sodium pyrophosphate decahydrate ($Na_4P_2O_7.10H_2O$), wet sieved, then treated with 10% HCl acid and 30% H_2O_2 solution to remove carbonates and organics, respectively. The magnetic sub-fraction was then removed using a hand magnet and mineral density separation was conducted using heavy liquid lithium heteropolytungstate to isolate KF grains at $\rho < 2.58$ gcm^{-3}. Samples from the Sand Ramp site were treated with 48% hydrofluoric acid (HF) to remove the outer alpha-irradiating rind of the grains; this simplifies dose rate calculations. Treatment included a short HF etch for 10 minutes followed by a 10% HCl acid treatment for ~10 hours. These samples were then sieved to remove grains that were reduced to <180 μm by the HF etch. Samples from the KTM study site were not treated with HF, so the alpha contribution to their environmental dose rates was included in age calculations.

Equivalent dose determination

The equivalent dose (D_e) for all samples was measured using a modified single aliquot regenerative-dose (SAR) technique (Murray and Wintle, 2000, 2003) designed for the post-IRIR_{225} signal (e.g., Rhodes, 2015) (Table S1). Steps 1-9 of the protocol constitute one SAR cycle. The first SAR cycle measures the sensitivity corrected natural signal, and subsequent SAR cycles measure the regenerative-dose signals (Lx/Tx) after a series of successively increasing laboratory radiation doses administered to the sample. The regeneration doses are used to generate a dose-response curve (i.e., Lx/Tx vs regenerative dose) onto which the natural signal (Ln/Tn) is plotted to calculate the D_e value. Regeneration doses include one "zero-dose" point where no radiation dose is given to measure recuperation, and one "repeat-dose" point, where a previous regeneration dose is measured a second time to calculate the recycling ratio. See Murray and Wintle (2000; 2003) for details.

Samples from the KTM site (CL-16-1 through CL-16-10) were dated using multi-grain aliquots of ~70 180-250 μm grains each and samples collected from the Sand ramp site (CL-14-1, CL-14-2) were measured using single 180-250 μm grains. Multi-grain aliquot signal measurements (Steps 3, 4, 7 and 8 in Table S1) were conducted with a cluster of Vishay TSFF 5210 IR diodes with peak emission at 870 nm, maximum power of 145 mW/cm^2 at the sample position, and

Corning/Kopp 7-59 and Schott BG39 filters transmitting 320-460 nm. Single grain IR stimulation (Steps 4 and 8, Table S1) was made with a 150 mW IR laser emitting 830 nm wavelength filtered with RG780, Corning/Kopp 7-59, and Schott BG39 filters transmitting 320-460 nm. For single grains, signal measurements during Steps 3 and 7 were conducted using the Vishay IR diodes and Corning/Kopp 7-59 and Schott BG39 filters mentioned above. Ln, Lx, Tn and Tx measurements included an IR stimulation duration of 100 s for multi-grain aliquots and 1.0 s for single grains.

Table S1. The post-$IRIR_{225}$ SAR dating protocol used in this study[1].

Step	Sample treatment
1	Natural/Regenerative Dose
2	Preheat (250°C, 60 s)
3	IR stimulation (50°C, 100 s)
4	IR stimulation (225°C) → L_n, L_x
5	Test dose (~7 Gy)
6	Preheat (250°C, 60 s)
7	IR stimulation (50°C, 100 s)
8	IR stimulation (225°C) → T_n, T_x
9	IR stimulation (290°C, 40 s)
10	Return to step 1.

[1]Ln = natural signal, Lx = regenerative dose signal. Tn = test dose signal measured after Ln, Tx = test dose signal measured after Lx.

Single-grain and single-aliquot dose-response curves were fitted to a saturating exponential function of the form:

$$I = I_0 + I_{Max}(1 - e^{-D/D_0}) \quad (1)$$

where I is the luminescence signal that increases with applied dose (D), D_0 is the characteristic saturation dose, I_0 is the initial offset of the signal from zero, and I_{Max} is the upper limit to the luminescence signal intensity. Routine screening criteria included rejection of multi-grain aliquots or single grains that exhibited the following behavior and characteristics:

- dim signals, as judged from net natural signals less than three standard deviations above the background,
- natural signals that did not intersect the dose-response curves,
- failure to produce, to within 10%, the same signal intensity from identical regeneration doses given at the beginning and end of the SAR sequence, which suggests inaccurate sensitivity correction (i.e., recycling ratios outside of 10% of unity),
- a test dose error of > 10%, and

- recuperation > 10% of the natural signal for ancient samples and >5% of the highest regenerative dose signal for sunbleached samples used for the bleaching test (below).

D_e distributions were plotted as kernel density estimates and radial plots and examined for outlying D_e values and asymmetry that may be attributed to incomplete bleaching (Fig. S1).

Dose rate determination

Samples for dose rate measurement were dried and milled to a fine, flour consistency and sent to ALS Geochemistry in Reno, NV for determination of U, Th and K_2O contents. Rb was not measured but rather was estimated based on sample K concentrations using the suggested 270:1 ratio of Mejdahl (1987). Samples used for U and Th content measurements were fused with lithium borate and measured with ICP-MS. K_2O was measured on bulk sample with ICP-AES and converted to % K. Total dose rates (Gy/ka) include an internal dose rate of 0.9 ± 0.1 Gy/ka to take into account an assumed internal K content of 12.5 ± 0.5 % within KF grains (Huntley and Baril, 1997). This internal dose rate has been scaled for a grain size of 180-250 μm in DRAC (Durcan et al., 2015). Total dose rates were calculated using DRAC (Durcan et al., 2015) using the conversion factors of Liritzis et al. (2013) and are shown to 2 decimal places (Table S2). A maximum water content of 2 ± 1 % (expressed as the percentage of the mass of dry sediment) was used in age calculations for all samples except for CL-16-10, which was estimated to be 20 ± 10% owing to the field measured water content and lacustrine origin. Cosmic dose rates (Gy/ka) were calculated according to Prescott and Hutton (1994).

Environmental dose rate data

Table S1. Dose rate data for luminescence samples in this study.

Sample	Study site	Depth (m)	U (ppm)	Th (ppm)	K (%)	Alpha dose rate (Gy/ka)	Beta dose rate (Gy/ka)	Gamma dose rate (Gy/ka)	Cosmic dose rate (Gy/ka)	Total dose rate (Gy/ka)
CL-16-1	KTM	1.0	2.42	6.24	2.19	0.052 ± 0.015	2.037 ± 0.166	1.108 ± 0.068	0.208 ± 0.021	3.41 ± 0.18
CL-16-2	KTM	1.2	2.46	7.29	2.28	0.055 ± 0.016	2.081 ± 0.172	1.159 ± 0.073	0.202 ± 0.020	3.50 ± 0.19
CL-16-3	KTM	0.5	2.68	6.14	2.22	0.053 ± 0.016	2.056 ± 0.168	1.122 ± 0.070	0.238 ± 0.024	3.47 ± 0.18
CL-16-4	KTM	0.5	2.74	12.75	2.13	0.079 ± 0.023	2.119 ± 0.164	1.406 ± 0.088	0.241 ± 0.024	3.85 ± 0.19
CL-16-5	KTM	0.3	2.28	4.91	2.39	0.045 ± 0.013	2.119 ± 0.179	1.070 ± 0.069	0.254 ± 0.025	3.49 ± 0.19
CL-16-6	KTM	0.4	2.0	6.68	2.41	0.049 ± 0.014	2.137 ± 0.180	1.128 ± 0.072	0.246 ± 0.025	3.56 ± 0.20
CL-16-7	KTM	0.5	2.84	7.00	1.97	0.058 ± 0.017	1.881 ± 0.151	1.104 ± 0.069	0.241 ± 0.024	3.28 ± 0.17
CL-16-8	KTM	0.6	2.08	4.05	2.30	0.039 ± 0.011	2.010 ± 0.172	0.985 ± 0.065	0.231 ± 0.023	3.27 ± 0.19
CL-16-9	KTM	1.0	2.04	5.74	2.25	0.045 ± 0.013	1.999 ± 0.168	1.045 ± 0.067	0.209 ± 0.021	3.30 ± 0.18
CL-16-10	KTM	1.4	3.38	12.85	2.22	0.070 ± 0.022	1.888 ± 0.231	1.272 ± 0.137	0.198 ± 0.020	3.43 ± 0.27
CL-14-1	Sand Ramp	1.0	1.50	4.30	3.41	N/A	2.680 ± 0.243	1.20 ± 0.087	0.210 ± 0.021	4.09 ± 0.26
CL-14-2	Sand Ramp	1.0	1.31	6.77	3.50	N/A	2.770 ± 0.250	1.32 ± 0.093	0.210 ± 0.021	4.30 ± 0.27

Fading correction

Fading measurements were conducted on a subset of samples using the SAR measurement procedure of Auclair et al. (2003) and the IRSL stimulation conditions and preheat temperatures in Table S1. In this procedure, samples were bleached, administered a known laboratory dose, preheated, then their sensitivity-corrected signals (Lx/Tx) were measured after a series of delay times ranging from ~1000 to ~600,000 s. Because feldspar IRSL signals fade in a log-linear fashion, fading rates are quantified using a g-value, which is the percent decrease in signal intensity per decade, where a decade refers to a 10-fold increase in delay time (Huntley and Lamothe, 2001).

For the KTM study site samples, we measured fading rates from 10 aliquots of sample CL-16-4 and used the resulting weighted mean g-value (0.95 ± 0.33) to correct the ages of samples CL-16-1 through CL-16-9 for fading using the model of Huntley and Lamothe (2001). Sample CL-16-10 has a different depositional history, and unique luminescence properties from the other samples at the KTM site. Therefore, we corrected the age of this sample using its own measured fading rate of 1.25 ± 0.43 %/decade. Luminescence ages from samples collected from the Sand Ramp site was corrected using a weighted mean g-value of 1.14 ± 0.61 %/decade that was measured from 28 individual grains from sample CL-14-2.

Bleaching test

A bleaching test was conducted on 20 aliquots of K-feldspar aliquots from sample CL-16-6 to assess the likelihood that the post-$IRIR_{225}$ signal was sufficiently exposed to sunlight prior to burial at the KMT and Sand Ramp sites. Aliquots were exposed directly to sunlight for durations of 0 s, 10 s, 1000 s, 10,000 s and 100,000 s (4 aliquots per duration), then measured using the SAR protocol in Table S1 (Fig. S2). After 10,000 s (2.8 h) the post-$IRIR_{225}$ signal decreased to 5% of its initial natural signal, and after 100,000 s (27.8 h) the signal was reduced to negligible levels.

CL-16-1

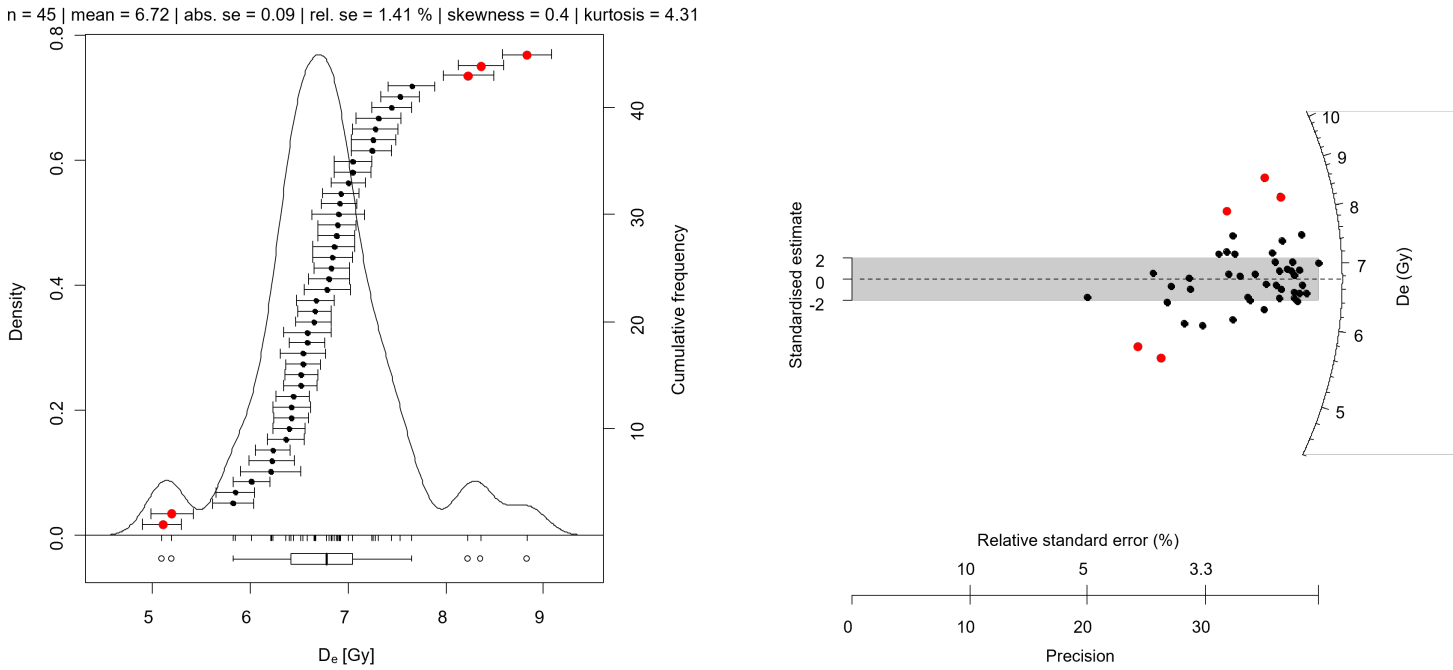

Figure S1. Kernel density estimate (left) and radial plots (right) for all sample De distributions. Plots were generated using the Luminescence Package in R (Kreutzer et al., 2012; 2021). All radial plots are centered on the CAM weighted mean De value, and points that lie within the shaded region are within 2 standard deviations of the CAM weighted mean. Read points are outliers that have been removed prior to final age calculation.

CL-16-2

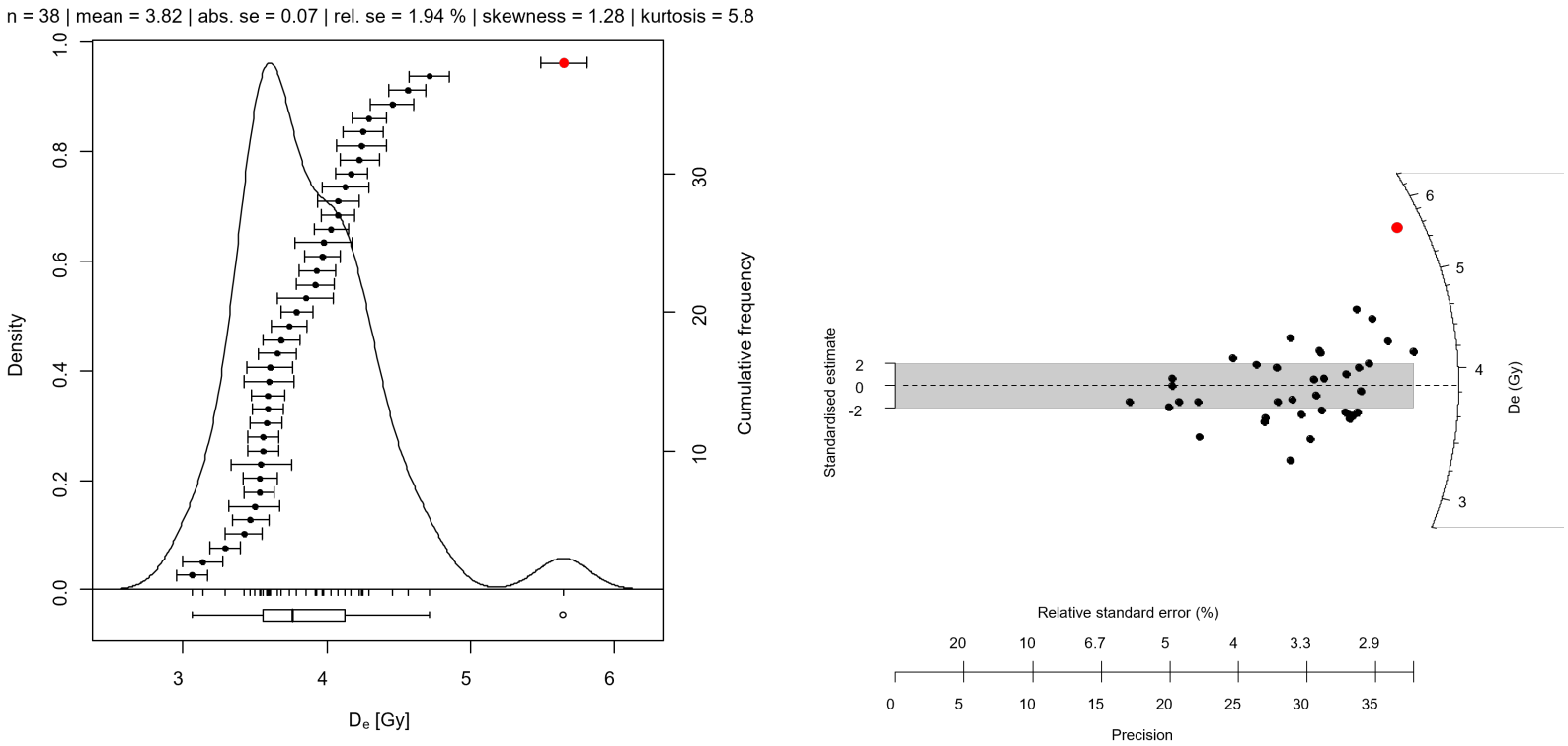

Figure S1, continued.

CL-16-3

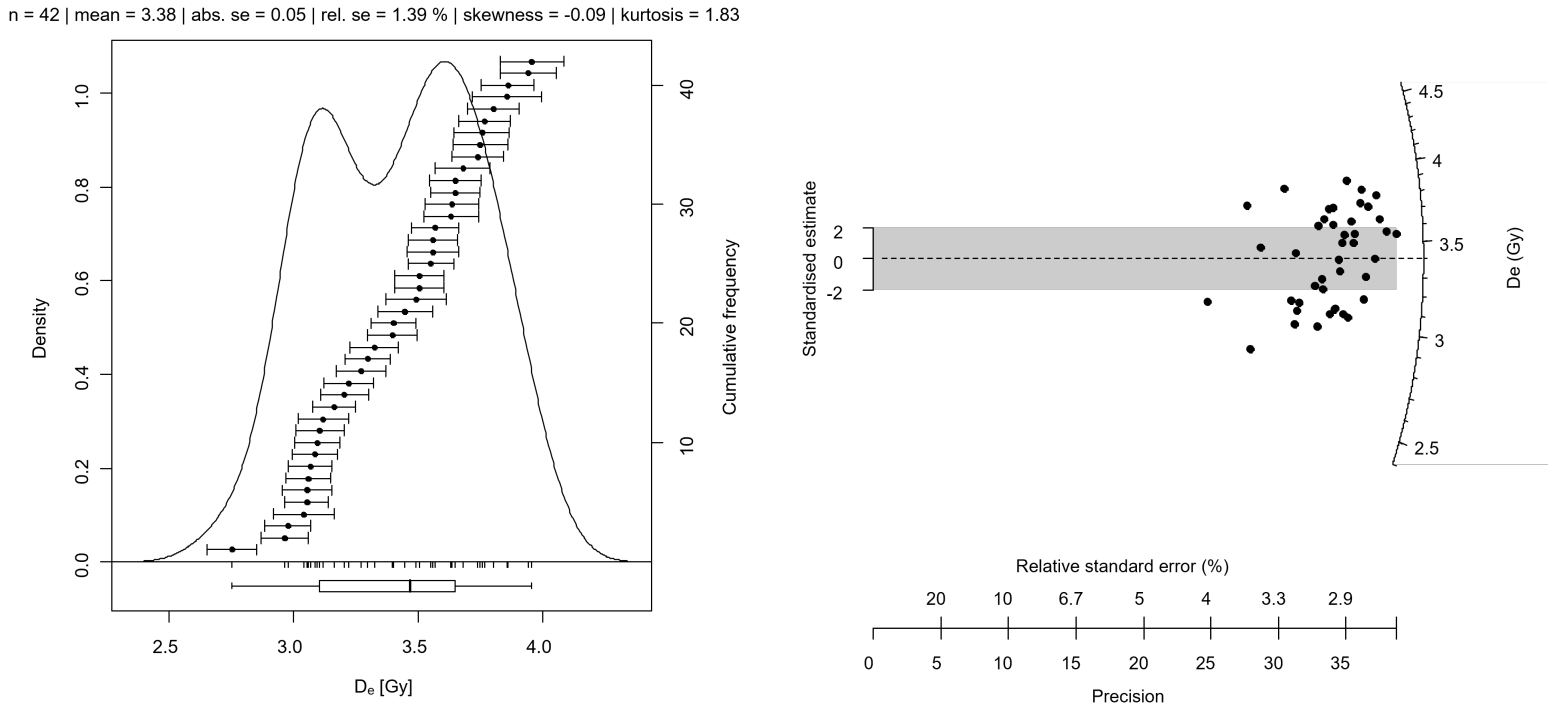

Figure S1, continued.

CL-16-4

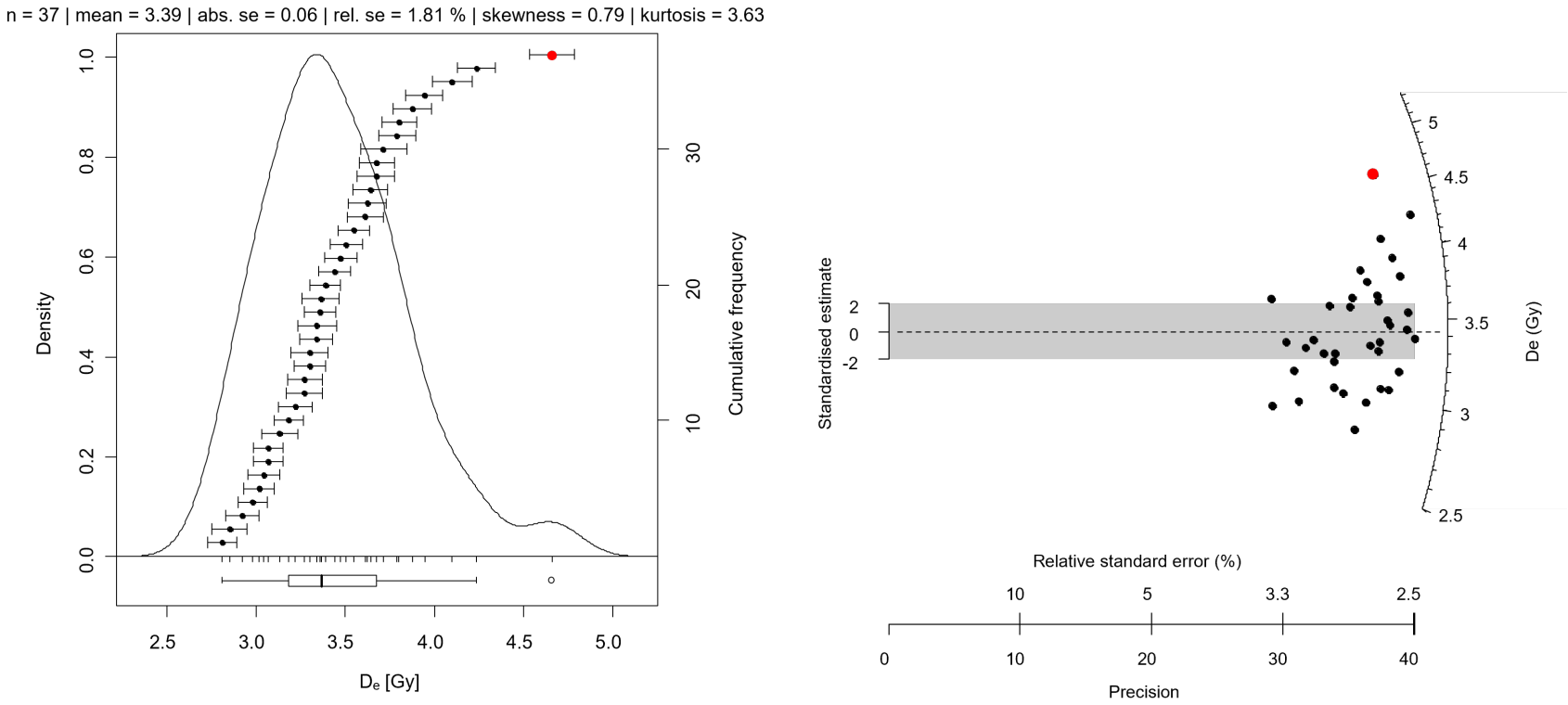

Figure S1, continued.

CL-16-5

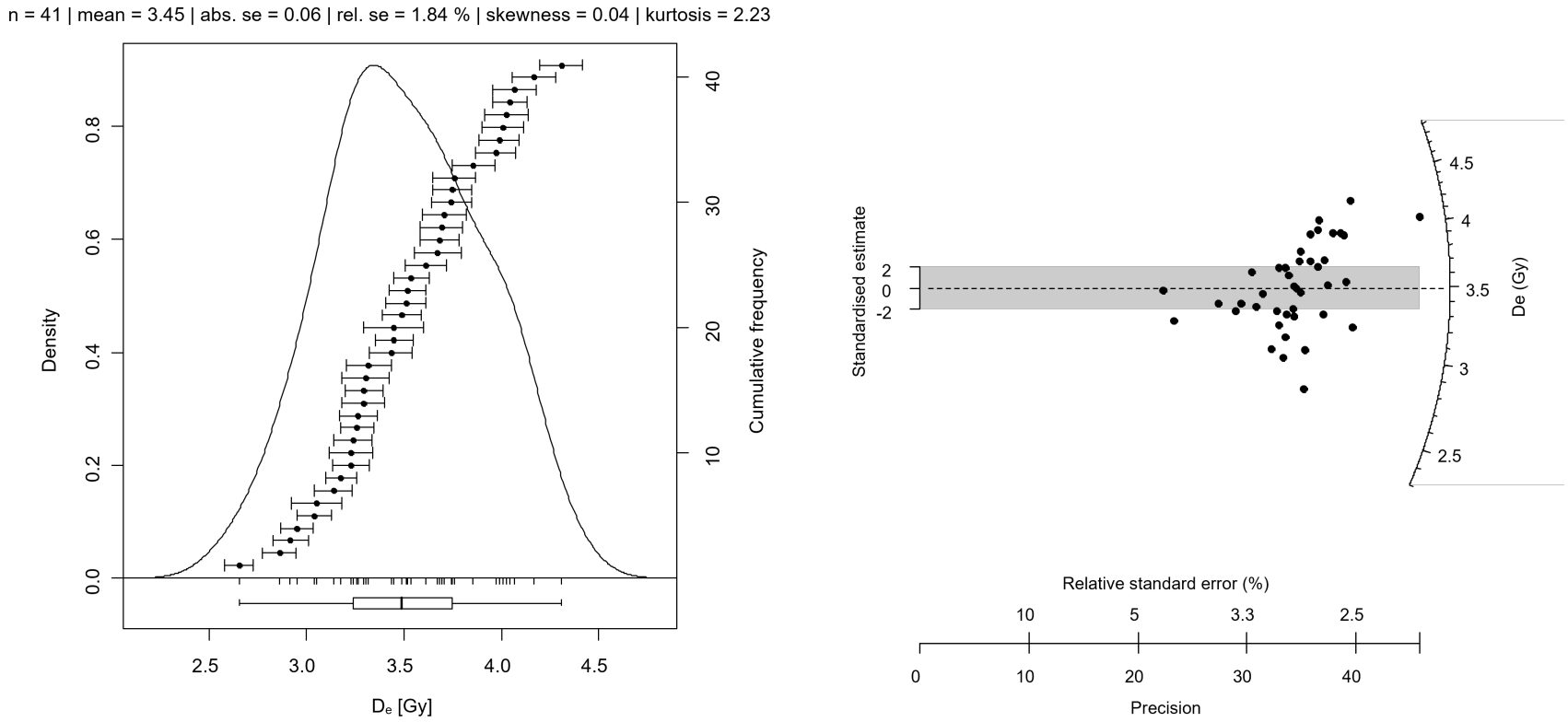

Figure S1, continued.

CL-16-6

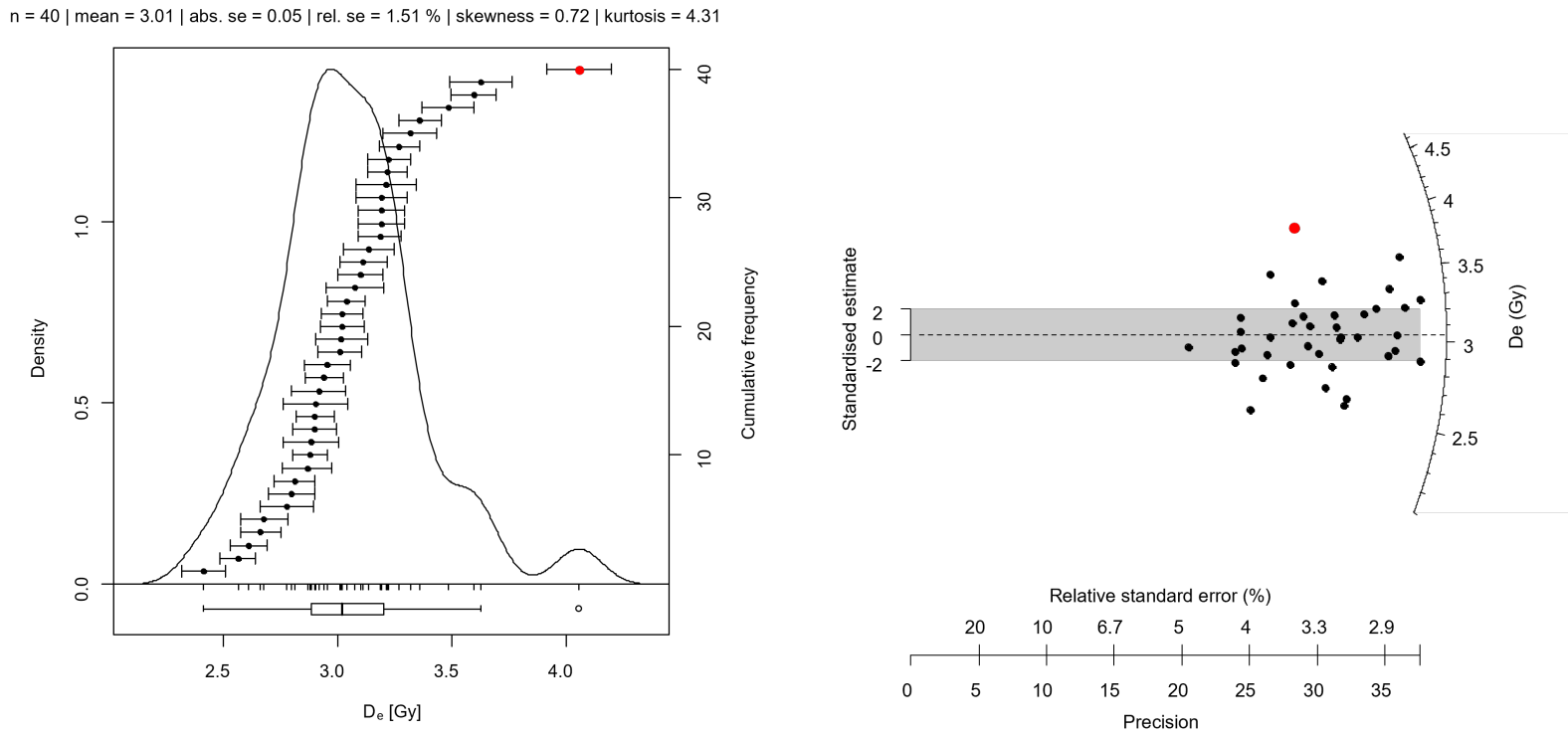

Figure S1, continued.

CL-16-7

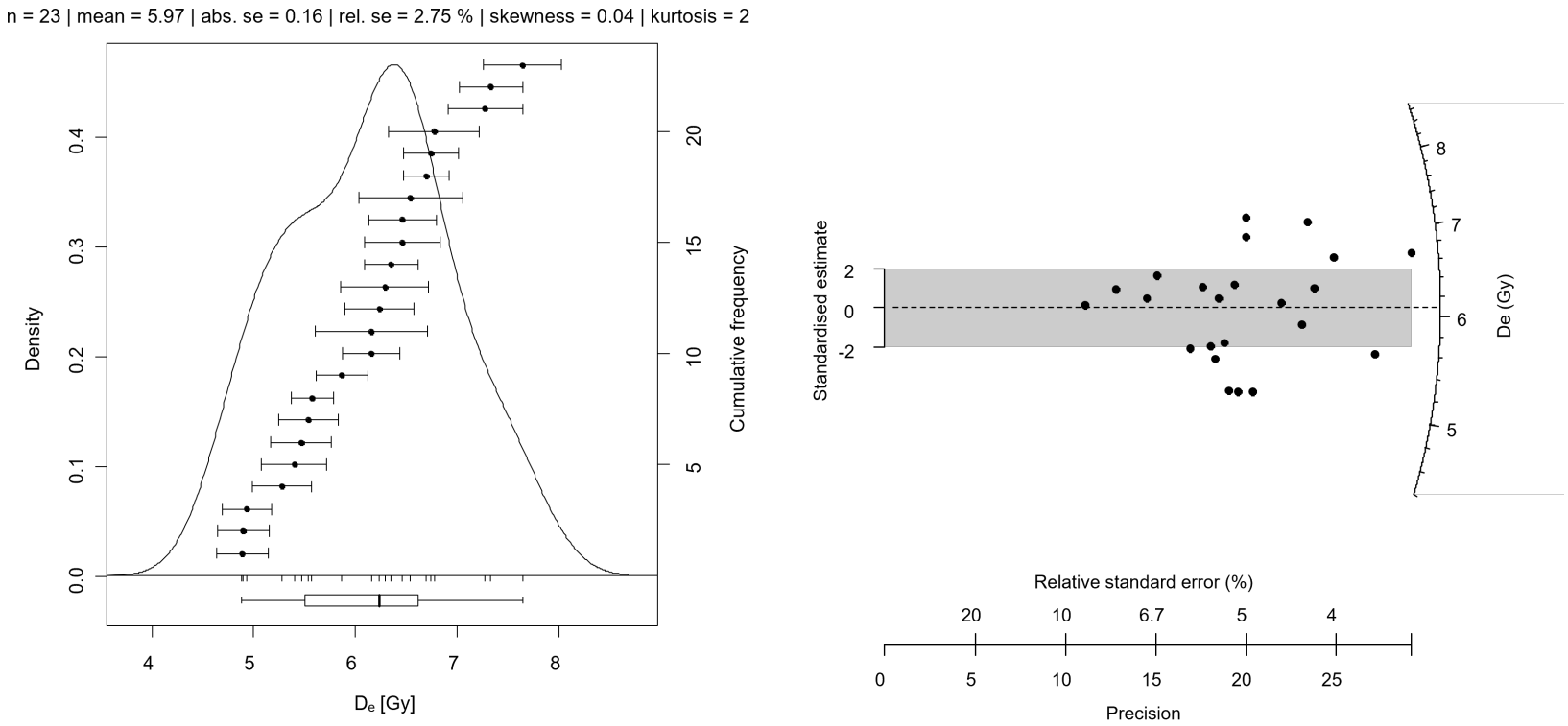

Figure S1, continued.

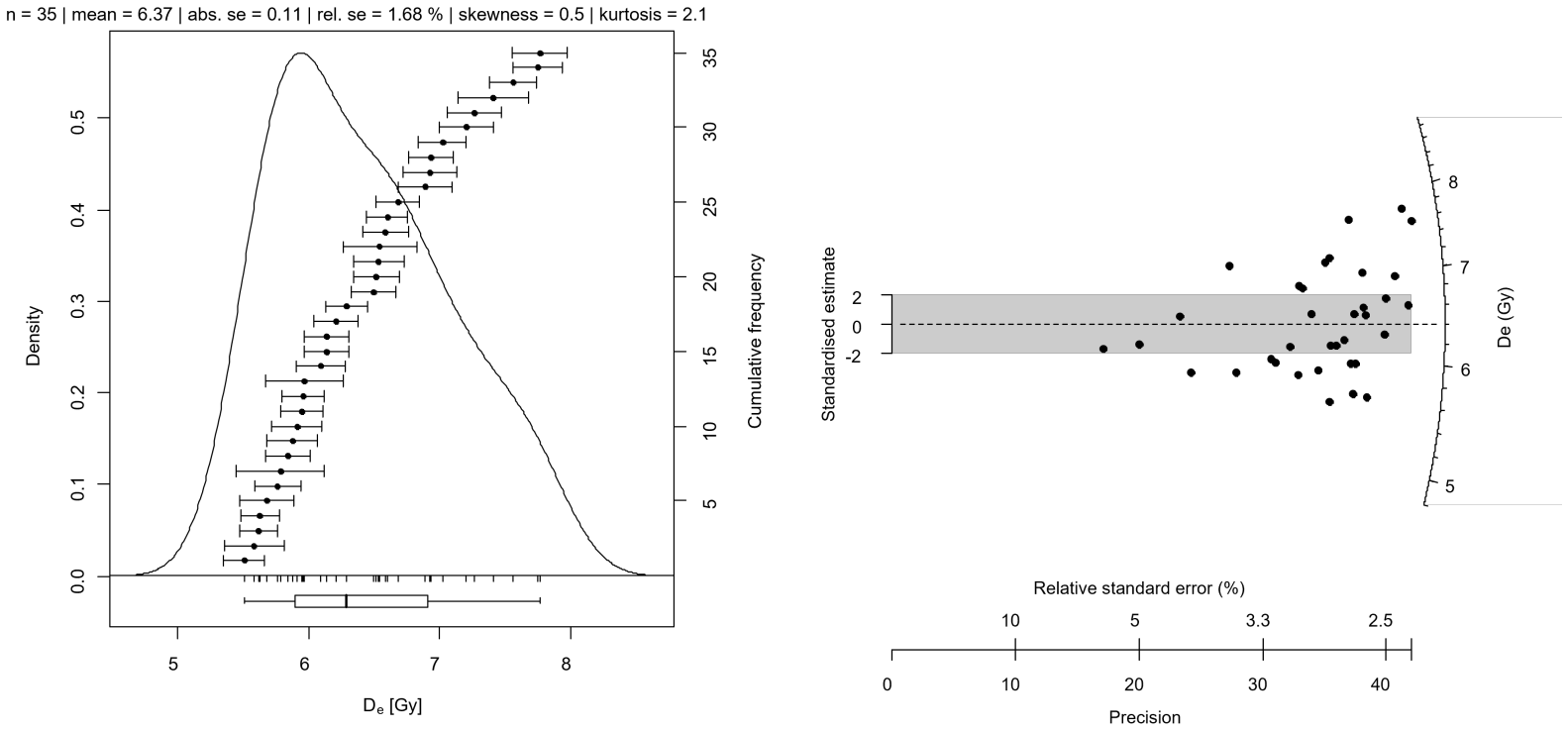

Figure S1, continued.

CL-16-9

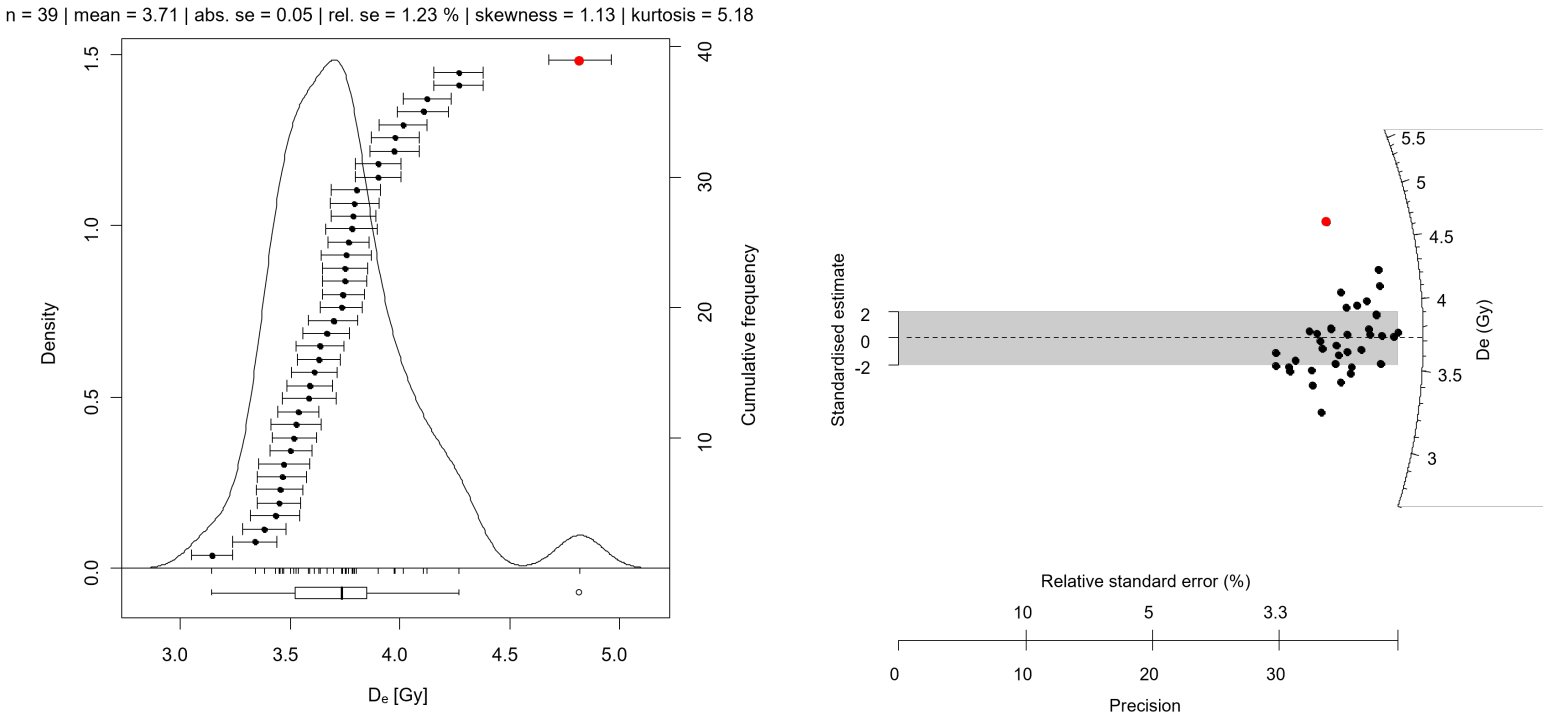

Figure S1, continued.

CL-16-10

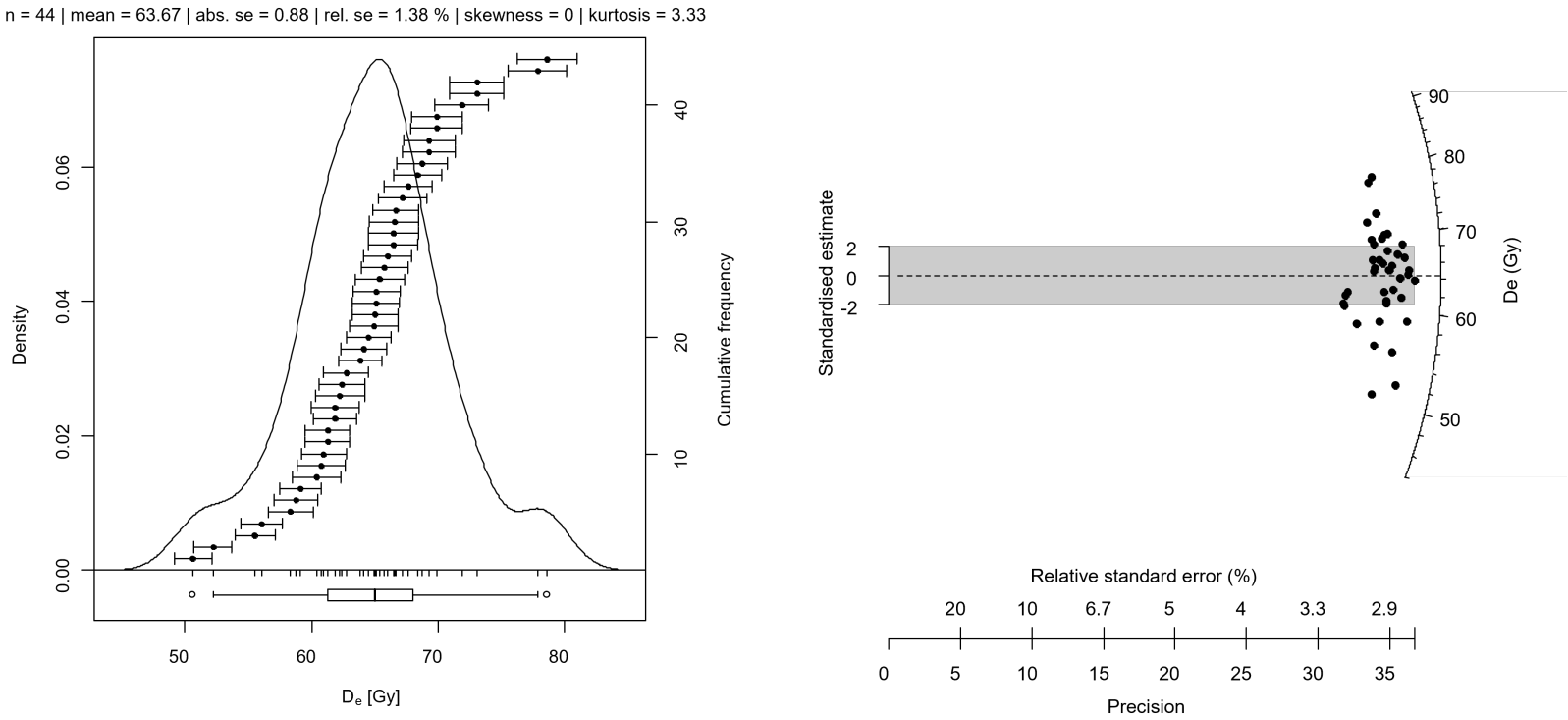

Figure S1, continued.

CL-14-1

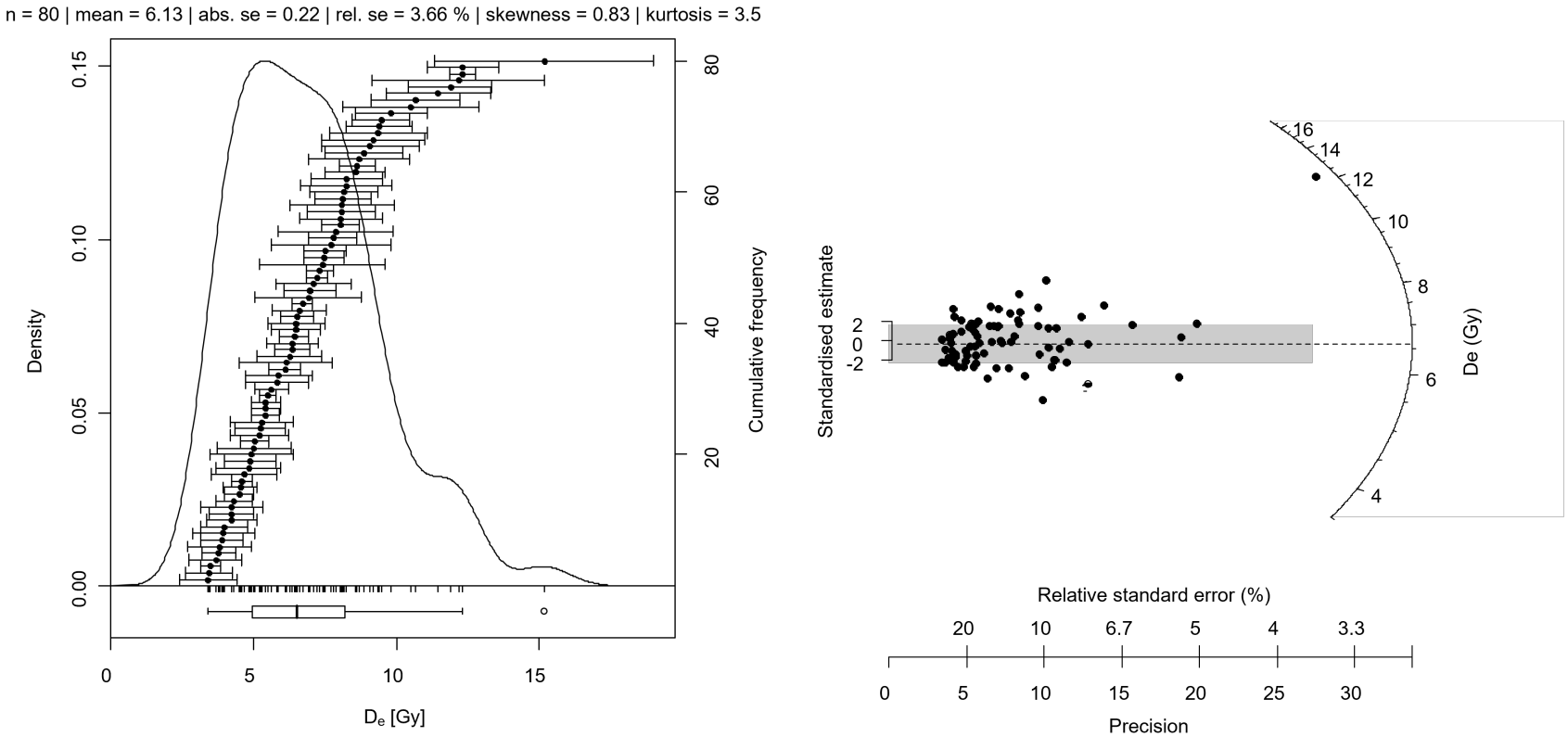

Figure S1, continued.

CL-14-2

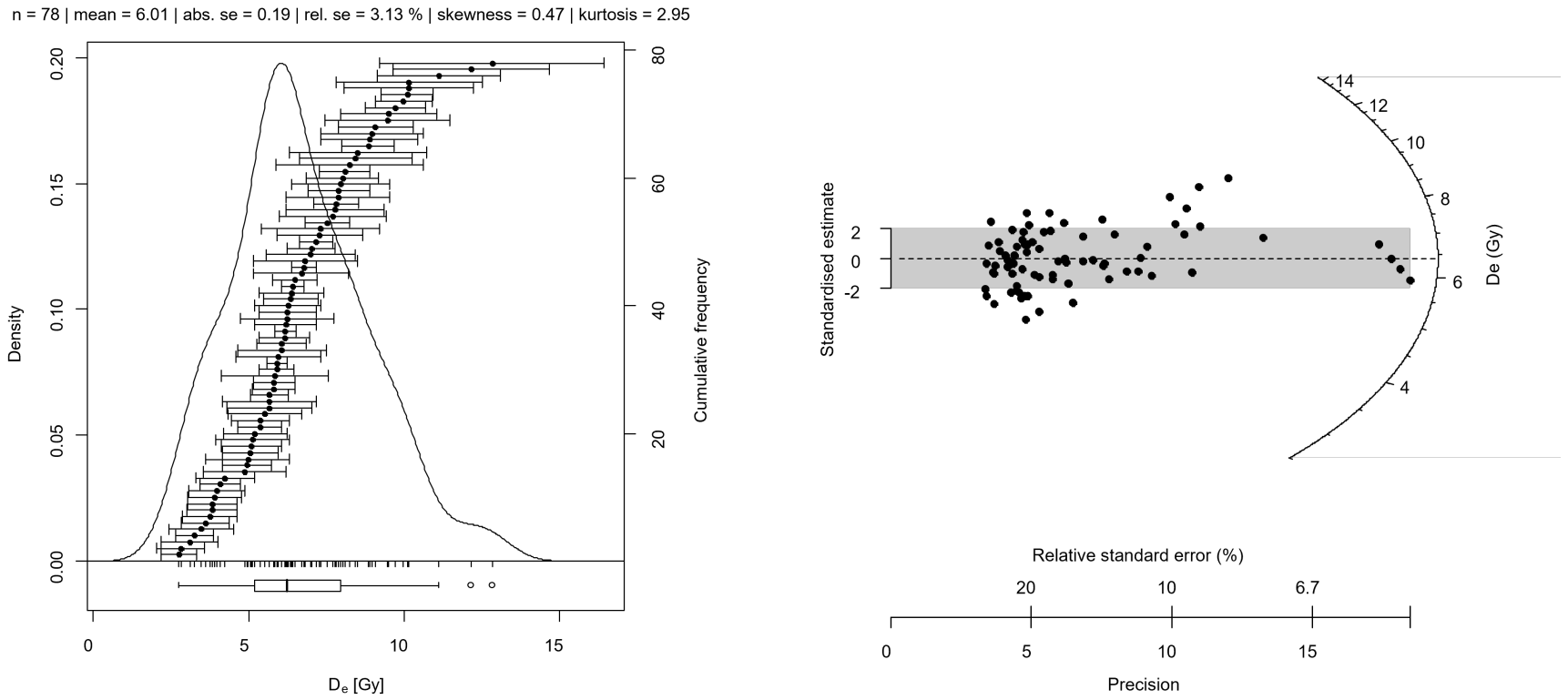

Figure S1, continued.

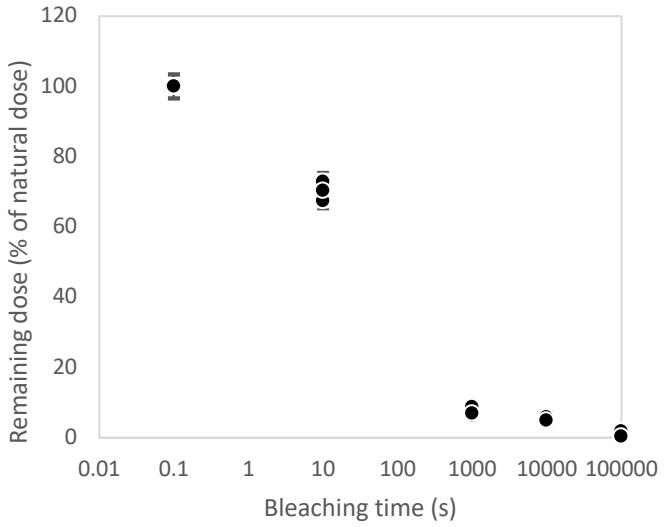

Figure S2. Bleaching test results on K-feldspar aliquots from sample CL-16-6. Bleaching times are plotted on a log scale and aliquots that were bleached for 0 s are plotted at 0.1 s for clarity.

REFERENCES

Aitken, M. J. & Smith, B. W., 1988. Optical dating: Recuperation after bleaching. Quaternary Science Reviews 7, 387–393.

Auclair, M., Lamothe, M. & Huot, S., 2003. Measurement of anomalous fading for feldspar IRSL using SAR. Radiation Measurements 37, 487–492.

Durcan, J.A., King, G.E., and Duller, G.A.T., 2015. DRAC: Dose rate and age calculator for trapped charge dating. Quaternary Geochronology 28, 54–61.

Galbraith, R. F., Roberts, R. G., Laslett, G. M., Yoshida, H. & Olley, J. M., 1999. Optical dating of single and multiple grains of quartz from Jinmium rock shelter, northern Australia: Part I, experimental design and statistical models. Archaeometry 41, 339–364.

Huntley, D. J. & Baril, M. R., 1997. The K content of the K-feldspars being measured in optical dating or in thermoluminescence dating. Ancient TL 15, 11–13.

Huntley, D. J. & Lamothe, M., 2001. Ubiquity of anomalous fading in K-feldspars and the measurement and correction for it in optical dating. Canadian Journal of Earth Sciences 38, 1093–1106.

Kreutzer S., Burow C., Dietze M., Fuchs M., Schmidt C., Fischer M., Friedrich J., Mercier N., Philippe A., Riedesel S., Autzen M., Mittelstrass D., Gray H., 2021. Luminescence: Comprehensive Luminescence Dating Data Analysis. R package version 0.9.13, https://CRAN.R-project.org/package=Luminescence.

Kreutzer S., Schmidt C., Fuchs M.C., Dietze M., Fischer M., Fuchs M. (2012). "Introducing an R package for luminescence dating analysis." Ancient TL 30(1), 1–8.

Liritzis, I., Singhvi, A. K., Feathers, J.K., Wagner, G.A., Kadereit, A., Zacharias, N., Li, S-H., 2013. Luminescence Dating in Archaeology, Anthropology, and Geoarchaeology – An Overview. Springer Briefs in Earth System Sciences. 70 pp.

Mejdahl, V., 1987. Internal radioactivity in quartz and feldspar grains. Ancient TL 5, 10–17.

Prescott, J.R., & Hutton, J.T., 1994. Cosmic ray contributions to dose rates for luminescence and ESR dating: large depths and long-term time variations. Radiation Measurements 23, 497–500.

Rhodes, E.J., 2015. Dating sediments using potassium feldspar single-grain IRSL: initial methodological considerations. Quaternary International 362, 14–22.